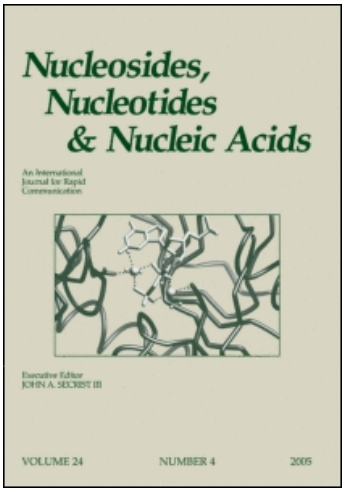

Nucleosides, Nucleotides and Nucleic Acids
Publication details, including instructions for authors and subscription information:
http://www.informaworld.com/smpp/title~content=t713597286

Interrupted 2'-*O*,4'-*C*-Aminomethylene Bridged Nucleic Acid Modification Enhances Pyrimidine Motif Triplex-Forming Ability and Nuclease Resistance Under Physiological Condition

Hidetaka Torigoe[a]; S. M. Abdur Rahman[b]; Hiroko Takuma[b]; Norihiro Sato[a]; Takeshi Imanishi[b]; Satoshi Obika[b]; Kiyomi Sasaki[a]
[a] Department of Applied Chemistry, Faculty of Science, Tokyo University of Science, Tokyo, Japan [b] Graduate School of Pharmaceutical Sciences, Osaka University, Osaka, Japan

Online publication date: 22 January 2011

Nucleosides, Nucleotides and Nucleic Acids, 30:63–81, 2011

ISSN: 1525-7770 print / 1532-2335 online
DOI: 10.1080/15257770.2010.543118

INTERRUPTED 2′-*O*,4′-*C*-AMINOMETHYLENE BRIDGED NUCLEIC ACID MODIFICATION ENHANCES PYRIMIDINE MOTIF TRIPLEX-FORMING ABILITY AND NUCLEASE RESISTANCE UNDER PHYSIOLOGICAL CONDITION

Hidetaka Torigoe,[1] S. M. Abdur Rahman,[2] Hiroko Takuma,[2] Norihiro Sato,[1] Takeshi Imanishi,[2] Satoshi Obika,[2] and Kiyomi Sasaki[1]

[1]*Department of Applied Chemistry, Faculty of Science, Tokyo University of Science, Tokyo, Japan*

[2]*Graduate School of Pharmaceutical Sciences, Osaka University, Osaka, Japan*

□ *Due to instability of pyrimidine motif triplex DNA at physiological pH, triplex stabilization at physiological pH is crucial in improving its potential in various triplex formation-based strategies in vivo, such as regulation of gene expression, mapping of genomic DNA, and gene-targeted mutagenesis. To this end, we investigated the effect of our previously reported chemical modification, 2′-O,4′-C-aminomethylene bridged nucleic acid (2′,4′- BNA^{NC}) modification, introduced into interrupted and continuous positions of triplex-forming oligonucleotide (TFO) on pyrimidine motif triplex formation at physiological pH. The interrupted 2′,4′-BNA^{NC} modifications of TFO increased the binding constant of the triplex formation at physiological pH by more than 10-fold, and significantly increased the nuclease resistance of TFO. On the other hand, the continuous 2′,4′-BNA^{NC} modification of TFO showed lower ability to promote the triplex formation at physiological pH than the interrupted 2′,4′-BNA^{NC} modifications of TFO, and did not significantly change the nuclease resistance of TFO. Selection of the interruptedly 2′,4′-BNA^{NC}-modified positions in TFO was more favorable for achieving the higher binding affinity of the pyrimidine motif triplex formation at physiological pH and the higher nuclease resistance of TFO than that of the continuously 2′,4′-BNA^{NC}-modified positions in TFO. We conclude that the interrupted 2′,4′-BNA^{NC} modification of TFO could be a key chemical modification to enhance pyrimidine motif triplex-forming ability and nuclease resistance under physiological condition, and may eventually lead to progress in various triplex formation-based strategies in vivo.*

Received 30 August 2010; accepted 23 November 2010.

This work was supported in part by Grant-in-Aid for Scientific Research on Innovative Areas (22113519 to H. T.), Grant-in-Aid for Exploratory Research (20655038 to S. O.), Grant-in-Aid for Scientific Research (B) (21350094 to S. O.), and Grant-in-Aid for JSPS Fellows (22-10383 to K. S.) from the Ministry of Education, Science, Sports, and Culture of Japan. This work was also supported partly by the Program for Promotion of Fundamental Studies in Health Sciences of the National Institute of Biomedical Innovation (NIBIO).

Address correspondence to Hidetaka Torigoe, Department of Applied Chemistry, Faculty of Science, Tokyo University of Science, 1-3 Kagurazaka, Shinjuku-ku, Tokyo 162-8601, Japan. E-mail: htorigoe@rs.kagu.tus.ac.jp

Keywords triplex; 2′-*O*,4′-*C*-aminomethylene bridged nucleic acid; interrupted modification; triplex forming ability; nuclease resistance; thermodynamics; kinetics

INTRODUCTION

In recent years, triplex nucleic acid has attracted considerable interest because of its possible biological functions in vivo and its wide variety of potential applications in vivo, such as regulation of gene expression by antigene technology, mapping of genomic DNA, and gene-targeted mutagenesis.[1–5] A triplex nucleic acid is usually formed through the sequence-specific interaction between a single-stranded homopyrimidine or homopurine triplex-forming oligonucleotide (TFO) and the major groove of homopurine-homopyrimidine stretch in duplex DNA.[3,4] In the pyrimidine motif triplex, a homopyrimidine TFO binds parallel to the homopurine strand of the target duplex by Hoogsteen hydrogen bonding to form T•A:T and C^+•G:C base triplets.[3,4] On the other hand, in the purine motif triplex, a homopurine TFO binds antiparallel to the homopurine strand of the target duplex by reverse Hoogsteen hydrogen bonding to form A•A:T (or T•A:T) and G•G:C base triplets.[3,4]

Because protonation of the cytosine bases in a homopyrimidine TFO is required to bind with the guanine bases of the G:C target duplex, the formation of the pyrimidine motif triplex needs an acidic pH condition and is, thus, extremely unstable at physiological neutral pH.[6–8] On the other hand, the pH-independent formation of the purine motif triplex is available at neutral pH. However, the purine motif triplex formation is severely inhibited by physiological concentrations of certain monovalent cations, especially K^+.[9,10] Undefined association between K^+ and the guanine-rich homopurine TFO has been applied to explain the inhibitory effect.[9,10] Thus, stabilization of the pyrimidine motif triplex at neutral pH is quite necessary for improving the potential of the triplex in various triplex formation-based strategies in vivo. Replacement of the cytosine bases in a homopyrimidine TFO with 5-methylcytosine[7,11–13] or other chemically modified base analogues,[14–18] and conjugation of different DNA intercalators to TFO[19,20] have been used to overcome the requirement of an acidic pH for the pyrimidine motif triplex formation and to stabilize the pyrimidine motif triplex at neutral pH.

We first synthesized and developed a new class of chemical modifications of nucleic acids, 2′-*O*,4′-*C*-aminomethylene bridged nucleic acid (2′,4′-BNA^{NC}) (Figure 1a), in which 2′-O and 4′-C of the sugar moiety were bridged with the aminomethylene chain.[21,22] The thermal stability of the triplex with 2′,4′-BNA^{NC}-modified TFO at neutral pH was much higher than that with the corresponding natural phosphodiester TFO, which was shown by UV melting to analyze the dissociation process of the triplex.[21,22] However, the formation process of the triplex involving 2′,4′-BNA^{NC}-modified TFO has not

(a)

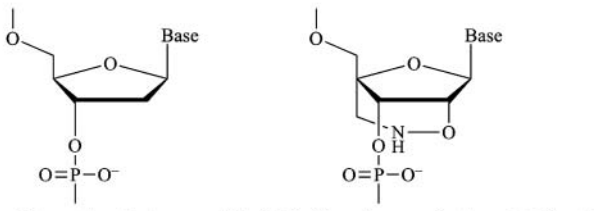

Phosphodiester (PO)

2'-*O*,4'-*C*-aminomethylene bridged nucleic acid (2',4'-BNA^{NC})

(b)

```
Pyr15TM           5′-CTCTTCTTTTCTTTC-3′
Pyr15BNANC5-1     5′-CTCTTCTTTTCTTTC-3′
Pyr15BNANC5-2     5′-CTCTTCTTTTCTTTC-3′
Pyr15BNANC5-3     5′-CTCTTCTTTTCTTTC-3′
Pur23A       5′-GCGCGAGAAGAAAAGAAAGCCGG-3′
Pyr23T       3′-CGCGCTCTTCTTTTCTTTCGGCC-5′
Pyr15NS2M         5′-TCTCTTCTTTTCTCT-3′
C: 5-methylcytosine
C: C with 2′-O,4′-C-aminomethylene bridge
T: T with 2′-O,4′-C-aminomethylene bridge
```

FIGURE 1 a) Structural formulas for phosphodiester (PO) and 2′-*O*,4′-*C*-aminomethylene bridged nucleic acid (2′,4′-BNA^{NC})-modified backbones. b) Oligonucleotide sequences for the target duplex (Pur23A•Pyr23T), the specific TFOs (Pyr15TM, Pyr15BNANC5-1, Pyr15BNANC5-2, and Pyr15BNANC5-3), and the nonspecific oligonucleotide (Pyr15NS2M).

been well-characterized yet. To explore the possibility for the application of 2′,4′-BNA^{NC}-modified TFO to the various triplex formation-based strategies in vivo, the investigation of the formation process of the triplex involving 2′,4′-BNA^{NC}-modified TFO may be more important than that of the dissociation process of the same triplex. In the present study, therefore, we have examined the effect of the 2′,4′-BNA^{NC} modification of TFO on the pyrimidine motif triplex formation at neutral pH. To investigate whether the difference in 2′,4′-BNA^{NC} modified positions may affect the ability of the pyrimidine motif triplex formation at neutral pH, we have used both the interruptedly and continuously 2′,4′-BNA^{NC}-modified TFOs. The effect of the interrupted and continuous 2′,4′-BNA^{NC} modifications on the pyrimidine motif triplex formation between a 23-base pair homopurine-homopyrimidine target duplex (Pur23A•Pyr23T) (Figure 1b) and each of its specific 15-mer 2′,4′-BNA^{NC}-unmodified homopyrimidine TFO (Pyr15TM) (Figure 1b), the corresponding interruptedly 2′,4′-BNA^{NC}-modified TFOs (Pyr15BNANC5-1 and Pyr15BNANC5-2) (Figure 1b), and the corresponding continuously 2′,4′-BNA^{NC}-modified TFO (Pyr15BNANC5-3) (Figure 1b) has been analyzed by electrophoretic mobility shift assay (EMSA),[23–29] isothermal titration calorimetry (ITC)[24–26,28,30–33] and BIACORE interaction

analysis system.[34,35] To explore the possibility for the application of 2′,4′-BNA^{NC}-modified TFOs in vivo, the resistance of each of the 2′,4′-BNA^{NC}-unmodified TFO and the corresponding interruptedly or continuously 2′,4′-BNA^{NC}-modified TFOs against nuclease degradation in human serum has been also investigated by anion-exchange high-performance liquid chromatography (HPLC). We have found that the interrupted 2′,4′-BNA^{NC} modifications of TFO increased the binding constant for the pyrimidine motif triplex formation at neutral pH by more than 10-fold. The continuous 2′,4′-BNA^{NC} modification of TFO also promoted the pyrimidine motif triplex formation at neutral pH, but it showed lower ability to promote the pyrimidine motif triplex at neutral pH than the interrupted 2′,4′-BNA^{NC} modifications of TFO. We have also revealed that the nuclease resistance of the interruptedly 2′,4′-BNA^{NC}-modified TFOs in human serum was significantly higher than that of the 2′,4′-BNA^{NC}-unmodified TFO. In contrast, the continuous 2′,4′-BNA^{NC} modification of TFO did not significantly change the nuclease resistance of the TFO. Thus, selection of the interruptedly 2′,4′-BNA^{NC}-modified positions in TFO was more favorable for the triplex-forming ability at neutral pH and the nuclease resistance of TFO than that of the continuously 2′,4′-BNA^{NC}-modified positions in TFO. The ability of the interrupted 2′,4′-BNA^{NC} modification to promote the pyrimidine motif triplex formation at neutral pH and achieve the significantly higher nuclease resistance of TFO under physiological condition would support further progress in the various triplex formation-based strategies in vivo.

EXPERIMENTAL

Preparation of Oligonucleotides

We synthesized 23-mer complementary oligonucleotides for the target duplex, Pur23A and Pyr23T (Figure 1b), a 15-mer 2′,4′-BNA^{NC}-unmodified homopyrimidine TFO with 5-methycytosine modification specific for the target duplex, Pyr15TM (Figure 1b), and a 15-mer nonspecific homopyrimidine oligonucleotide with 5-methycytosine modification, Pyr15NS2M (Figure 1b), on an ABI DNA synthesizer using the solid-phase cyanoethyl phosphoramidite method, and purified them with a reverse-phase HPLC on a Wakosil DNA column. The 15-mer interruptedly 2′,4′-BNA^{NC}-modified homopyrimidine TFOs, Pyr15BNANC5-1 and Pyr15BNANC5-2 (Figure 1b), and the 15-mer continuously 2′,4′-BNA^{NC}-modified homopyrimidine TFO, Pyr15BNANC5-3 (Figure 1b), with 5-methycytosine modification specific for the target duplex were synthesized and purified as described previously.[21,22] 5′-biotinylated Pyr23T (Bt-Pyr23T) was prepared using biotin phosphoramidite. The concentration of all oligonucleotides was determined by UV absorbance. Complementary strands, Pur23A and Pyr23T, were annealed by heating at up to 90°C, followed by a gradual cooling to room

temperature. The annealed sample was applied on a hydroxyapatite column (BIORAD Inc. USA) to remove unpaired single strands. The concentration of the duplex DNA (Pur23A•Pyr23T) was determined by UV absorption considering the DNA concentration ratio of 1 OD = 50 μg/ml, with a M_r of 15180.

EMSA

EMSA experiments were performed essentially as described previously by a 15% native polyacrylamide gel electrophoresis.[24–29]

ITC

Isothermal titration experiments were carried out on a VP ITC system (Microcal Inc., USA), essentially as described previously.[24–26,28] The TFO and Pur23A•Pyr23T duplex solutions were prepared by extensive dialysis against buffer A (10 mM sodium cacodylate-cacodylic acid at pH 6.8 containing 200 mM NaCl and 20 mM $MgCl_2$) or buffer B (10 mM sodium cacodylate-cacodylic acid at pH 6.1 containing 200 mM NaCl and 20 mM $MgCl_2$). The Pur23A•Pyr23T duplex solution in buffer A or buffer B was injected 20-times in 5 μl increments and 10 minute intervals into the TFO solution without changing the reaction conditions. The heat for each injection was subtracted by the heat of dilution of the injectant, which was measured by injecting the Pur23A•Pyr23T duplex solution into the same buffer. Each corrected heat was divided by the moles of the Pur23A•Pyr23T duplex solution injected, and analyzed with Microcal Origin software supplied by the manufacturer.

BIACORE Interaction Analysis System

Kinetic experiments were performed on a BIACORE J instrument (GE Healthcare, USA), in which a real-time biomolecular interaction was measured with a laser biosensor.[34,35] The layer of a SA sensor tip with immobilized streptavidin was equilibrated with buffer A at a flow rate of 30 μl/min. 40 μl of 50 mM NaOH containing 1 M NaCl was injected 3 times at a flow rate of 30 μl/min to reduce electrostatic repulsion from the surface. After equilibrating with buffer A, 160 μl of 0.2 μM Bt-Pyr23T•Pur23A duplex solution was added at a flow rate of 30 μl/min to bind with the streptavidin on the surface. After extensive washing and equilibrating the Bt-Pyr23T•Pur23A-immobilized surface with buffer A, 70 μl of the TFO solution in buffer A was injected over the immobilized Bt-Pyr23T•Pur23A duplex at a flow rate of 30 μl/min, and then the triplex formation was monitored for 2 minutes. This was followed by washing the sensor tip with buffer A, and the dissociation of the preformed triplex was monitored for an additional 2.5 minutes. Finally, 40 μl of 100 mM Tris-HCl (pH 8.0) for Pyr15TM, or 40 μl of 10 mM

NaOH (pH 12) for Pyr15BNANC5-1, Pyr15BNANC5-2, and Pyr15BNANC5-3 was injected at a flow rate of 30 μl/min to completely break the Hoogsteen hydrogen bonding between the TFO and Pur23A, during which the Bt-Pyr23T•Pur23A duplex may be partially denatured. The Bt-Pyr23T•Pur23A duplex was regenerated by injecting 0.2 μM Pur23A. The resulting sensorgrams were analyzed with the BIA evaluation software supplied by the manufacturer to calculate the kinetic parameters.

CD Spectroscopy

CD spectra at 20°C were recorded in buffer A on a JASCO J-720 spectropolarimeter interfaced with a microcomputer. The cell path length was 1 cm. The triplex nucleic acid concentration used was 1 μM.

Stability of TFO in Human Serum Analyzed by Anion-Exchange HPLC

An amount of 1 nmol TFO was incubated at 37°C in 20 μl of 50% human serum from human male AB plasma (Sigma-Aldrich Co., USA). After incubation for 20, 60, and 120 minutes, the samples were mixed with 13 μl of formamide to terminate the reactions, and stored at −80°C until HPLC analyses. The samples were mixed with 400 μl of HPLC buffer [25 mM Tris-HCl (pH 7.0), 0.5% CH_3CN], and analyzed by anion-exchange HPLC on JASCO LC-2000 Plus series with detection at 260 nm using a linear gradient of 0–0.5 M NH_4Cl in HPLC buffer over 45 minutes to resolve the products. The HPLC column used was TSK-GEL DNA-NPR (Tosoh, Japan). Under these conditions, peaks of all proteins from the human serum could be resolved from those of the intact and degraded TFO. Degradation data from the acquired chromatograms were processed using ChromNAV software as supplied by the manufacturer.

RESULTS

EMSA of Pyrimidine Motif Triplex Formation at Neutral pH

The pyrimidine motif triplex formation of the target duplex (Pur23A•Pyr23T; Figure 1b) with each of its specific 2′,4′-BNA^{NC}-unmodified TFO (Pyr15TM; Figure 1b), the interruptedly 2′,4′-BNA^{NC}-modified TFOs (Pyr15BNANC5-1 and Pyr15BNANC5-2; Figure 1b), and the continuously 2′,4′-BNA^{NC}-modified TFO (Pyr15BNANC5-3; Figure 1b) was examined at pH 7.0 by EMSA (Figure 2). Total oligonucleotide concentration ([specific TFO (Pyr15TM, Pyr15BNANC5-1, Pyr15BNANC5-2, or Pyr15BNANC5-3; Figure 1b)] + [nonspecific oligonucleotide (Pyr15NS2M; Figure 1b)]) was kept constant at 1 μM to minimize loss of DNA during processing and to assess sequence specificity. While incubation with 1 μM Pyr15NS2M alone did not cause a shift in electrophoretic migration of the target duplex (see lane 1 for

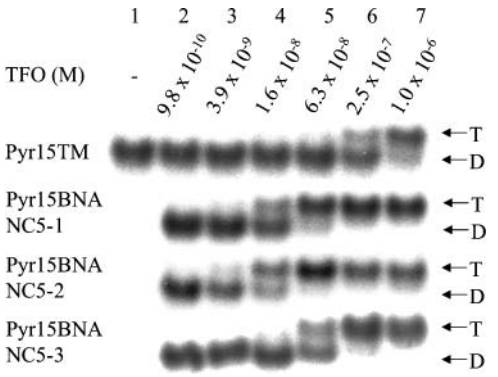

FIGURE 2 EMSA of the pyrimidine motif triplex formation with each of the specific TFO (Pyr15TM, Pyr15BNANC5-1, Pyr15BNANC5-2, and Pyr15BNANC5-3) at neutral pH. Triplex formation was initiated by adding ^{32}P-labeled Pur23A•Pyr23T duplex (~1 nM) with the indicated final concentrations of the specific TFO (Pyr15TM, Pyr15BNANC5-1, Pyr15BNANC5-2, and Pyr15BNANC5-3). The nonspecific oligonucleotide (Pyr15NS2M) was added to adjust the equimolar concentrations (1 μM) of TFO (Pyr15TM+Pyr15NS2M, Pyr15BNANC5-1+Pyr15NS2M, Pyr15BNANC5-2+Pyr15NS2M, and Pyr15BNANC5-3+Pyr15NS2M) in each lane. Reaction mixtures involving each of Pyr15TM, Pyr15BNANC5-1, Pyr15BNANC5-2 and Pyr15BNANC5-3 in 50 mM Tris-acetate (pH 7.0), 100 mM NaCl, and 10 mM $MgCl_2$ were incubated for 6 hours at 37°C, and then electrophoretically separated at 4°C on a 15% native polyacrylamide gel prepared in buffer [50 mM Tris-acetate (pH 7.0) and 10 mM $MgCl_2$]. Positions of the duplex (D) and triplex (T) are indicated.

Pyr15TM), those with each of Pyr15TM, Pyr15BNANC5-1, Pyr15BNANC5-2, and Pyr15BNANC5-3 at particular concentrations caused retardation of the duplex migration owing to triplex formation.[23] The dissociation constant, K_d, of triplex formation was determined from the concentration of the TFO, which caused half of the target duplex to shift to the triplex.[23] The K_d of the triplex with Pyr15TM was estimated to be between 0.25 and 1 μM. In contrast, the K_d of the triplex with each of Pyr15BNANC5-1 and Pyr15BNANC5-2 was ~0.016 μM, indicating that the interrupted 2′,4′-BNA^{NC} modification of TFO increased the binding constant, K_a ($=1/K_d$), of the pyrimidine motif triplex formation at neutral pH by more than 16-fold. On the other hand, the K_d of the triplex with Pyr15BNANC5-3 was ~0.063 μM, indicating that the continuous 2′,4′-BNA^{NC} modification of TFO increased the K_a of the pyrimidine motif triplex formation at neutral pH by only 4-fold. The magnitude of the increase in K_a by the continuous 2′,4′-BNA^{NC} modification of TFO was smaller than that by the interrupted 2′,4′-BNA^{NC} modification of TFO.

Thermodynamic Analyses of Pyrimidine Motif Triplex Formation by ITC

We examined the thermodynamic parameters of the pyrimidine motif triplex formation between a 23-base pair target duplex (Pur23A•Pyr23T) and each of its specific 15-mer 2′,4′-BNA^{NC}-unmodified TFO (Pyr15TM), the interruptedly 2′,4′-BNA^{NC}-modified TFOs (Pyr15BNANC5-1 and

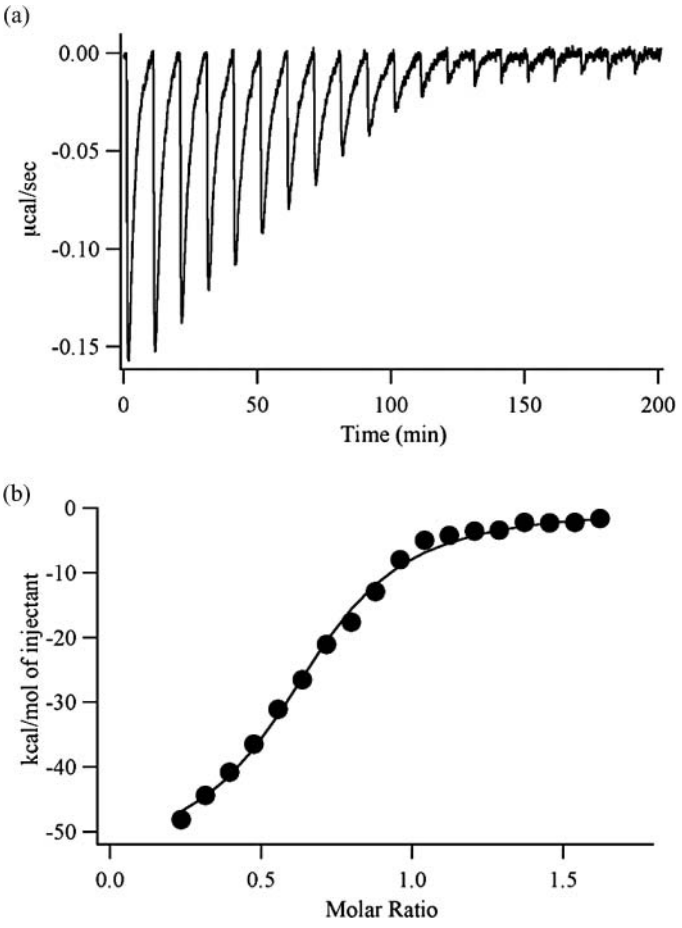

FIGURE 3 Thermodynamic analyses of the pyrimidine motif triplex formation involving Pyr15BNANC5-1 at 25°C and pH 6.8 by ITC. a) Typical ITC profiles for the triplex formation between Pyr15BNANC5-1 and Pur23A•Pyr23T at 25°C and pH 6.8. 114.7 μM Pur23A•Pyr23T solution in buffer A (See Experimental Section) was injected 20 times in 5-μl increments into 3.59 μM Pyr15BNANC5-1 solution, which was dialyzed against the same buffer. Injections were occurred over 12 seconds at 10-minutes intervals. b) The titration plot against the molar ratio of [Pur23A•Pyr23T]/[Pyr15BNANC5-1]. The data were fitted by a nonlinear least-squares method.

Pyr15BNANC5-2), and the continuously 2′,4′-BNA^{NC}-modified TFO (Pyr15BNANC5-3) at 25°C and pH 6.8 by ITC. To investigate the pH dependence of the pyrimidine motif triplex formation, the thermodynamic parameters of the pyrimidine motif triplex formation between Pur23A•Pyr23T and Pyr15TM were also analyzed at 25°C and pH 6.1 by ITC. Figure 3a shows a typical ITC profile for the triplex formation between Pyr15BNANC5-1 and Pur23A•Pyr23T at 25°C and pH 6.8. An exothermic heat pulse was observed after each injection of Pur23A•Pyr23T into Pyr15BNANC5-1. The magnitude of each peak decreased gradually with each new injection, and a small peak was still observed at a molar ratio of the last injection. The area of the small

peak was equal to the heat of dilution measured in a separate experiment by injecting Pur23A•Pyr23T into the same buffer. The area under each peak was integrated, and the heat of dilution of Pur23A•Pyr23T was subtracted from the integrated values. The corrected heat was divided by the moles of injected solution, and the resulting values were plotted as a function of a molar ratio of [Pur23A•Pyr23T]/[Pyr15BNANC5-1], as shown in Figure 3b. The resultant titration plot was fitted to a sigmoidal curve by a nonlinear least-squares method. The binding constant, K_a, and the enthalpy change, ΔH, were obtained from the fitted curve.[32] The Gibbs free energy change, ΔG, and the entropy change, ΔS, were calculated from the equation, $\Delta G = -RT\ln K_a = \Delta H - T\Delta S$, where R is gas constant and T is temperature.[32] The thermodynamic parameters for the pyrimidine motif triplex formation involving each of Pyr15TM, Pyr15BNANC5-2 and Pyr15BNANC5-3 at 25°C and pH 6.8 and those involving Pyr15TM at 25°C and pH 6.1 were obtained in the same way.

Table 1 summarizes the K_a values for the pyrimidine motif triplex formation with each of Pyr15TM, Pyr15BNANC5-1, Pyr15BNANC5-2, and Pyr15BNANC5-3 at 25°C and pH 6.8 and those with Pyr15TM at 25°C and pH 6.1, obtained from ITC. The K_a for Pyr15TM at pH 6.1 was ~10-fold larger than that observed for Pyr15TM at pH 6.8, confirming, like others,[6–8] that neutral pH is unfavorable for the pyrimidine motif triplex formation involving C^+•G:C triads. In addition, the K_a for each of Pyr15BNANC5-1 and Pyr15BNANC5-2 was ~10-fold larger than that observed for Pyr15TM (Table 1), indicating that the interrupted 2′,4′-BNA^{NC} modification of TFO increased the K_a for the pyrimidine motif triplex formation at neutral pH, which is consistent with the results of EMSA (Figure 2). In contrast, the K_a for Pyr15BNANC5-3 was only 3-fold larger than that observed for Pyr15TM (Table 1). The magnitude of the increase in K_a by the continuous 2′,4′-BNA^{NC} modification of TFO was smaller than that by the interrupted 2′,4′-BNA^{NC} modification of TFO, which is also consistent with the results of EMSA (Figure 2).

TABLE 1 Thermodynamic parameters for the triplex formation between a 23-base pair target duplex (Pur23A•Pyr23T) and a 15-mer TFO (Pyr15TM, Pyr15BNANC5-1, Pyr15BNANC5-2 or Pyr15BNANC5-3) at 25°C, obtained from ITC

TFO	pH	K_a (M^{-1})	K_a (relative)	ΔG (kcal mol^{-1})	ΔH (kcal mol^{-1})	ΔS (cal $mol^{-1}K^{-1}$)
Pyr15TM	6.1[a]	$(5.81 \pm 0.99) \times 10^6$	13.9	-9.23 ± 0.11	-92.0 ± 1.5	-278 ± 5
Pyr15TM	6.8[b]	$(4.19 \pm 2.0) \times 10^5$	1.0	-7.67 ± 0.38	-38.5 ± 7.5	-103 ± 26
Pyr15BNANC5-1	6.8[b]	$(3.73 \pm 0.43) \times 10^6$	8.9	-8.96 ± 0.07	-54.3 ± 1.5	-152 ± 5
Pyr15BNANC5-2	6.8[b]	$(3.82 \pm 0.29) \times 10^6$	9.1	-8.98 ± 0.05	-53.8 ± 1.1	-150 ± 4
Pyr15BNANC5-3	6.8[b]	$(1.18 \pm 0.10) \times 10^6$	2.8	-8.28 ± 0.05	-55.2 ± 1.4	-157 ± 4

[a]10 mM sodium cacodylate-cacodylic acid (pH 6.1), 200 mM NaCl and 20 mM $MgCl_2$.
[b]10 mM sodium cacodylate-cacodylic acid (pH 6.8), 200 mM NaCl and 20 mM $MgCl_2$.

Kinetic Analyses of Pyrimidine Motif Triplex Formation at Neutral pH by BIACORE Interaction Analysis System

To examine the putative mechanism involved in the increase in K_a of the pyrimidine motif triplex formation by the 2′,4′-BNA^{NC} modification of TFO (Figure 2 and Table 1), we assessed the kinetic parameters for the association and dissociation of TFO (Pyr15TM and the 2′,4′-BNA^{NC}-modified TFOs) with Pur23A•Pyr23T at 25°C and pH 6.8 by BIACORE. Figure 4a shows the sensorgrams representing the triplex formation and dissociation involving the

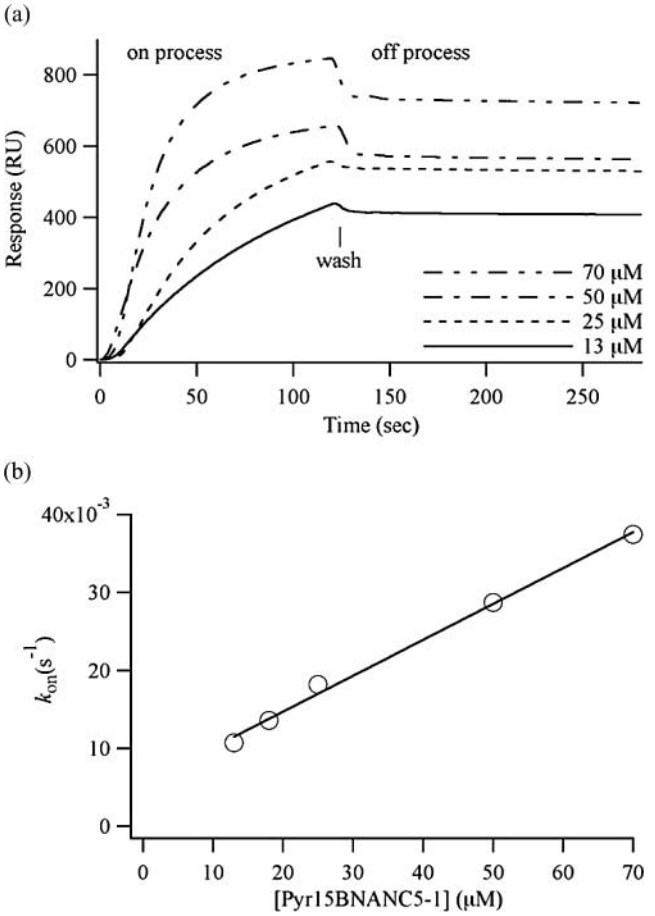

FIGURE 4 Kinetic analyses of the pyrimidine motif triplex formation involving Pyr15BNANC5-1 at 25°C and pH 6.8 by BIACORE interaction analysis system. a) A series of sensorgrams for the triplex formation and the dissociation of the formed triplex between Pyr15BNANC5-1 and Pur23A•Pyr23T at 25°C and pH 6.8. The Pyr15BNANC5-1 solutions, diluted in the buffer A to achieve the indicated final concentrations, were injected into the Bt-Pyr23T•Pur23A-immobilized cuvette. The binding of Pyr15BNANC5-1 to Bt-Pyr23T•Pur23A and the dissociation of Pyr15BNANC5-1 from Bt-Pyr23T•Pur23A were monitored as the response against time. b) Measured on-rate constants, k_{on}, of the triplex formation in (a) were plotted against the respective concentrations of Pyr15BNANC5-1. The plot was fitted to a straight line ($r^2 = 0.99$) by a linear least-squares method.

various concentrations of Pyr15BNANC5-1. The injection of Pyr15BNANC5-1 over the immobilized Bt-Pyr23T•Pur23A caused an increase in response. As shown in Figure 4a, an increase in the concentration of Pyr15BNANC5-1 led to a gradual change in the response of the association curves. The on-rate constant (k_{on}) was obtained from the analysis of each association curve. Figure 4b shows a plot of k_{on} against the Pyr15BNANC5-1 concentrations. The resultant plot was fitted to a straight line by a linear least-squares method. The association rate constant (k_{assoc}) was determined from the slope of the fitted line.[34,35] The off-rate constant (k_{off}) was obtained from the analysis of each dissociation curve (Figure 4a). As k_{off} is usually independent of the concentration of the injected solution, the dissociation rate constant (k_{dissoc}) was determined by averaging k_{off} for several concentrations.[34,35] K_a was calculated from the equation, $K_a = k_{assoc}/k_{dissoc}$. The kinetic parameters for each of Pyr15TM and other 2′,4′-BNA^{NC}-modified TFOs were obtained in the same way.

Table 2 summarizes the kinetic parameters for the pyrimidine motif triplex formation with each of Pyr15TM and the 2′,4′-BNA^{NC}-modified TFOs at 25°C and pH 6.8, obtained from BIACORE. The magnitudes of K_a calculated from the ratio of k_{assoc} to k_{dissoc} (Table 2) were consistent with those obtained from ITC (Table 1). The K_a for each of the interruptedly 2′,4′-BNA^{NC}-modified TFOs at pH 6.8 was ~30-fold larger than that observed for Pyr15TM at pH 6.8, indicating that the interrupted 2′,4′-BNA^{NC} modification of TFO significantly increased the K_a of the pyrimidine motif triplex formation at neutral pH, which supported the results of EMSA (Figure 2) and ITC (Table 1). The interrupted 2′,4′-BNA^{NC} modification of TFO decreased k_{dissoc} by ~15-fold, while it moderately increased k_{assoc} by ~2-fold. On the other hand, the K_a for the continuously 2′,4′-BNA^{NC}-modified TFO at pH 6.8 was ~4-fold larger than that observed for Pyr15TM at pH 6.8. The continuous 2′,4′-BNA^{NC} modification of TFO decreased k_{dissoc} by ~2.7-fold, while it increased k_{assoc} by ~1.3-fold. Thus, the much larger K_a by the 2′,4′-BNA^{NC} modification of TFO resulted mainly from the decrease in k_{dissoc} rather than the increase in k_{assoc}.

CD Spectroscopy of Pyrimidine Motif Triplex at Neutral pH

To further characterize the triplexes involving each of the 2′,4′-BNA^{NC}-unmodified TFO (Pyr15TM), the interruptedly 2′,4′-BNA^{NC}-modified TFOs (Pyr15BNANC5-1 and Pyr15BNANC5-2), and the continuously 2′,4′-BNA^{NC}-modified TFO (Pyr15BNANC5-3), circular dichroism (CD) spectra of the triplexes were measured at 20°C and pH 6.8 (Figure 5). A significant negative band in the short-wavelength (210–220 nm) region was observed for all the profiles (Figure 5), confirming the triplex formation involving each TFO.[36] The overall shape of the CD spectra was quite similar among all the profiles (Figure 5), suggesting that no significant change may be induced in the

TABLE 2 Kinetic parameters for the triplex formation between a 23-base pair target duplex (Pur23A•Pyr23T) and a 15-mer TFO (Pyr15TM, Pyr15BNANC5-1, Pyr15BNANC5-2 or Pyr15BNANC5-3) at 25°C and pH 6.8,[a] obtained from BIACORE interaction analysis system

TFO	k_{assoc} (M^{-1} s^{-1})	k_{assoc} (relative)	k_{dissoc} (s^{-1})	k_{dissoc} (relative)	K_a (M^{-1})	K_a (relative)
Pyr15TM	$(2.01 \pm 0.11) \times 10^2$	1.0	$(1.05 \pm 0.29) \times 10^{-3}$	1.0	$(1.91 \pm 0.88) \times 10^5$	1.0
Pyr15BNANC5-1	$(4.60 \pm 0.18) \times 10^2$	2.3	$(9.36 \pm 1.29) \times 10^{-5}$	0.089	$(4.91 \pm 1.01) \times 10^6$	25.7
Pyr15BNANC5-2	$(4.30 \pm 0.67) \times 10^2$	2.1	$(6.61 \pm 0.81) \times 10^{-5}$	0.063	$(6.51 \pm 2.06) \times 10^6$	34.1
Pyr15BNANC5-3	$(2.68 \pm 0.13) \times 10^2$	1.3	$(3.89 \pm 0.57) \times 10^{-4}$	0.37	$(6.89 \pm 1.57) \times 10^5$	3.6

[a]10 mM sodium cacodylate-cacodylic acid (pH 6.8), 200 mM NaCl and 20 mM $MgCl_2$.

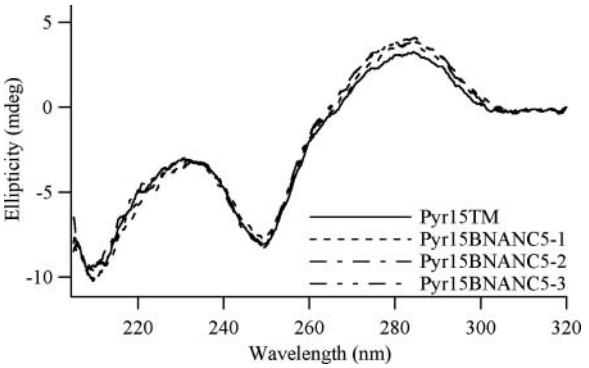

FIGURE 5 CD spectra of the pyrimidine motif triplexes with each of the specific TFO (Pyr15TM, Pyr15BNANC5-1, Pyr15BNANC5-2, and Pyr15BNANC5-3). The triplexes with each of Pyr15TM, Pyr15BNANC5-1, Pyr15BNANC5-2, and Pyr15BNANC5-3 in buffer A (see experimental section) were measured at 20°C in the wavelength range of 205–320 nm. The cell path length was 1 cm. The triplex nucleic acid concentration used was 1 μM.

higher-order structure of the pyrimidine motif triplex by the interrupted and continuous 2′,4′-BNA^{NC} modifications of TFO.

Stability of TFOs in Human Serum Against Nuclease Degradation

A major difficulty associated with the use of oligonucleotides as in vivo agents is the rapid degradation of oligonucleotides by nuclease in vivo.[37] To explore the possibility for the application of 2′,4′-BNA^{NC}-modified TFOs to the various triplex formation-based strategies in vivo, we examined the resistance of the 2′,4′-BNA^{NC}-unmodified TFO (Pyr15TM), the interruptedly 2′,4′-BNA^{NC}-modified TFOs (Pyr15BNANC5-1 and Pyr15BNANC5-2), and the continuously 2′,4′-BNA^{NC}-modified TFO (Pyr15BNANC5-3) against nuclease degradation by incubating the TFOs at 37°C in human serum and analyzing with anion-exchange HPLC. Figure 6 shows the percentage of the intact oligonucleotides as a function of the incubation time. Only 20–30% of intact Pyr15TM and Pyr15BNANC5-3 were detected after 20 minutes of incubation with human serum, and most of them were degraded within 60 minutes. The continuous 2′,4′-BNA^{NC} modification did not significantly change the nuclease resistance of TFO in human serum. In contrast, more than 50% of Pyr15BNANC5-1 and Pyr15BNANC5-2 remained intact even after 120 minutes of incubation with human serum. The interrupted 2′,4′-BNA^{NC} modification significantly increased the nuclease resistance of TFO in human serum.

DISCUSSION

The K_a of the pyrimidine motif triplex formation with each of Pyr15BNANC5-1 and Pyr15BNANC5-2 at pH 6.8 was ~10-fold larger than

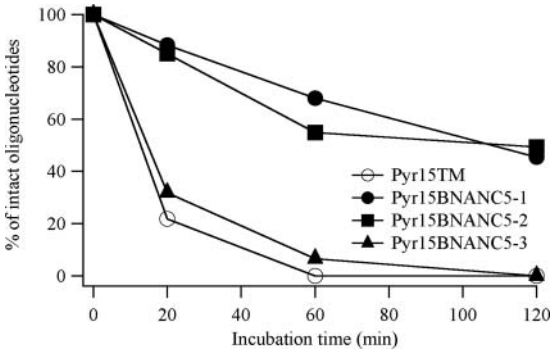

FIGURE 6 Stability of the specific TFOs (Pyr15TM, Pyr15BNANC5-1, Pyr15BNANC5-2, and Pyr15BNANC5-3) in human serum. 1 nmol TFOs were incubated in human serum at 37°C, and aliquots were removed at the time points indicated and analyzed by anion-exchange HPLC. The percentage of the intact oligonucleotides was determined and plotted as a function of the incubation time.

that observed with Pyr15TM at pH 6.8 (Table 1). The K_a of the pyrimidine motif triplex formation with Pyr15BNANC5-3 at pH 6.8 was 3-fold larger than that observed with Pyr15TM at pH 6.8 (Table 1). The increase in K_a at neutral pH by the 2′,4′-BNA^{NC} modifications of TFO was supported by the results of EMSA (Figure 2) and BIACORE (Table 2), although the magnitudes of the K_a ($=1/K_d$) values were different between EMSA (Figure 2) and each of ITC (Table 1) and BIACORE (Table 2) due to the difference in the experimental buffer conditions. Our previous UV melting study showed that the melting temperature of the triplex involving the singly 2′,4′-BNA^{NC}-modified TFO at neutral pH was significantly higher than that involving the unmodified TFO [21, 22], indicating that even the single 2′,4′-BNA^{NC} modification of TFO had the ability to increase the thermal stability of the triplex at neutral pH. The study also showed that the increase in the melting temperature of the triplex by the three interrupted 2′,4′-BNA^{NC} modification of TFO at neutral pH was a little higher than that by the three continuous 2′,4′-BNA^{NC} modification of TFO,[21,22] which was consistent with the present results. These results indicate that the 2′,4′-BNA^{NC} modification of TFO promotes the pyrimidine motif triplex formation at neutral pH, although the degree of the promotion at neutral pH were different between the interrupted and continuous 2′,4′-BNA^{NC} modifications of TFO.

The magnitudes of K_a for the interruptedly 2′,4′-BNA^{NC}-modified TFOs (Pyr15BNANC5-1 and Pyr15BNANC5-2) at pH 6.8 and that for Pyr15TM at pH 6.1 were similar and larger than that for Pyr15TM at pH 6.8 (Table 1), indicating the effective and stoichiometric triplex formations for the interruptedly 2′,4′-BNA^{NC}-modified TFOs at pH 6.8 and for Pyr15TM at pH 6.1. In contrast, the triplex formation involving Pyr15TM at pH 6.8 with the significantly smaller magnitude of K_a is less stoichiometric. Thus, the comparison of the thermodynamic parameters (ΔH and ΔS) between the

interruptedly 2′,4′-BNA^{NC}-modified TFOs at pH 6.8 and Pyr15TM at pH 6.8 is not valid due to the significantly reduced stoichiometry for Pyr15TM at pH 6.8. The comparison of ΔH and ΔS between the interruptedly 2′,4′-BNA^{NC}-modified TFOs at pH 6.8 and Pyr15TM at pH 6.1 with similar stoichiometry will provide a reasonable promotion mechanism for the triplex formation by the 2′,4′-BNA^{NC} modification. Although the magnitudes of K_a and ΔG for the interruptedly 2′,4′-BNA^{NC}-modified TFOs at pH 6.8 and for Pyr15TM at pH 6.1 were similar, the constituents of ΔG, that is ΔH and ΔS, were different from each other. The magnitudes of the negative ΔH and ΔS for the interruptedly 2′,4′-BNA^{NC}-modified TFOs at pH 6.8 were smaller than those observed for Pyr15TM at pH 6.1. The observed ΔS upon the triplex formation is mainly contributed by the two factors, a negative conformational entropy change due to the conformational restraint of TFO involved in the triplex formation, and a positive dehydration entropy change from the release of structured water molecules surrounding the TFO and the target duplex upon the triplex formation.[38–41] Therefore, one of the reason for the smaller magnitudes of the negative ΔS for the 2′,4′-BNA^{NC}-modified TFOs at pH 6.8 in comparison with that for Pyr15TM at pH 6.1 (Table 1) may be based on the negative conformational entropy change. Because the CD spectra showed that the higher-order structure of the formed triplexes with each of the 2′,4′-BNA^{NC}-modified TFOs was quite similar to that with Pyr15TM (Figure 5), the difference in the conformational entropy change should result from the structural difference between the unmodified and 2′,4′-BNA^{NC}-modified TFOs in the free state. The 2′,4′-BNA^{NC}-modified TFO in the free state may be more rigid than the corresponding unmodified TFO, because the 2′-O and 4′-C positions of the sugar moiety of the 2′,4′-BNA^{NC} are bridged with the aminomethylene chain. The increased rigidity of the 2′,4′-BNA^{NC}-modified TFO in the free state relative to the corresponding unmodified TFO may cause the smaller loss of the conformational entropy upon the binding of the 2′,4′-BNA^{NC}-modified TFO with the target duplex to form the triplex at neutral pH. Another reason for the smaller magnitudes of the negative ΔS for the 2′,4′-BNA^{NC}-modified TFOs at pH 6.8 relative to that for Pyr15TM at pH 6.1 (Table 1) may be derived from the positive dehydration entropy change. The nitrogen atom in the aminomethylene chain may result in the increased degree of hydration of the 2′,4′-BNA^{NC}-modified TFO in the free state relative to the corresponding unmodified TFO. The increased degree of hydration of the 2′,4′-BNA^{NC}-modified TFO in the free state may cause the larger gain of the dehydration entropy upon the binding of the 2′,4′-BNA^{NC}-modified TFO with the target duplex to form the triplex at neutral pH. These two possible reasons, the smaller loss of the conformational entropy and the larger gain of the dehydration entropy, may result in the more entropy gain for the 2′,4′-BNA^{NC}-modified TFO relative to the unmodified TFO, which provides a favorable component to the ΔG and leads to the increase in the K_a of the pyrimidine motif triplex formation at neutral

pH. Thus, the increased rigidity and the increased degree of hydration of the 2′,4′-BNA^{NC}-modified TFO in the free state may be important factors to increase the K_a of the pyrimidine motif triplex formation at neutral pH.

The nuclease resistance of the interruptedly 2′,4′-BNA^{NC}-modified TFO was significantly higher than that of the unmodified TFO, although the nuclease resistance of the unmodified and continuously 2′,4′-BNA^{NC}-modified TFOs was similar (Figure 6). The interrupted 2′,4′-BNA^{NC} modification increased the nuclease resistance of TFOs in human serum. Previously, the nuclease resistance of the phosphorothioate backbone, in which a nonbridging oxygen of a phosphodiester group was replaced by a sulfur atom, was known to be significantly higher than that of the unmodified backbone.[42,43] However, the K_a of the triplex formation with the phosphorothioate-modified TFO was significantly smaller than that with the unmodified TFO.[33,44] Thus, the phosphorothioate modification increased the nuclease resistance of TFO, but it decreased the triplex forming ability. On the other hand, as discussed above, the interrupted 2′,4′-BNA^{NC} modification of TFO increased the triplex forming ability at neutral pH (Figure 2 and Table 1). Therefore, the interrupted 2′,4′-BNA^{NC} modification enhanced both the nuclease resistance of TFO and the triplex forming ability at neutral pH. We conclude that due to these excellent properties the interrupted 2′,4′-BNA^{NC} modification may be more favorable than the phosphorothioate modification upon the application of TFO to the various triplex formation-based strategies in vivo.

The magnitude of the increase in K_a at neutral pH by the continuous 2′,4′-BNA^{NC} modification was significantly smaller than that by the interrupted 2′,4′-BNA^{NC} modification (Figure 2 and Table 1). In spite of the same number of the 2′,4′-BNA^{NC} modification, the pyrimidine motif triplex-forming ability at neutral pH was quite different between the interrupted and continuous 2′,4′-BNA^{NC} modifications. In the continuously 2′,4′-BNA^{NC}-modified TFO, the rigid region in the free state produced by the 2′,4′-BNA^{NC} modification discussed above may be limited around the continuously modified region of TFO, but the overall region of TFO may be rigid in the free state in the interruptedly 2′,4′-BNA^{NC} modified TFO due to the entire distribution of the modification. Thus, the conformational entropy loss due to the conformational restraint of TFO upon the binding with the target duplex may be larger for the continuously modified TFO. In fact, the magnitude of the negative ΔS for the continuously modified TFO was larger than that for the interruptedly modified TFOs (Table 1). The more entropy loss for the continuously modified TFO relative to the interruptedly modified TFO may provide an unfavorable component to the ΔG and lead to the decrease in the K_a of the pyrimidine motif triplex formation at neutral pH. On the other hand, although the interrupted 2′,4′-BNA^{NC} modification significantly increased the nuclease resistance of TFO, the continuous 2′,4′-BNA^{NC} modification did not significantly change the nuclease resistance of TFO (Figure 6). In spite of the same number of the 2′,4′-BNA^{NC} modification,

the nuclease resistance of TFO was quite different between the interrupted and continuous 2′,4′-BNA^{NC} modifications. In the interruptedly 2′,4′-BNA^{NC} modified TFO (Pyr15BNANC5-1 and Pyr15BNANC5-2), the positions near the 5′ and 3′ ends are modified with the 2′,4′-BNA^{NC} (Figure 1b) and may be resistant to the exonuclease in the human serum. However, the positions near the 5′ and 3′ ends are unmodified (Figure 1b) and may be easily hydrolyzed by the exonuclease in the continuously 2′,4′-BNA^{NC} modified TFO (Pyr15BNANC5-3). The absence and presence of the 2′,4′-BNA^{NC} modification near the 5′ and 3′ ends may be one of the important factors for the stability of TFOs in human serum against nuclease degradation in addition to the interrupted and continuous modifications. We conclude that the positions of the 2′,4′-BNA^{NC} modification in TFO significantly affected the pyrimidine motif triplex-forming ability at neutral pH and the nuclease resistance of TFO. The interrupted modification in TFO was more favorable for achieving the higher pyrimidine motif triplex-forming ability at neutral pH and the higher nuclease resistance of TFO than the continuous modification in TFO with the unmodified 5′ and 3′ ends.

The present study has clearly demonstrated that the interrupted 2′,4′-BNA^{NC} modification of TFO increased the K_a of the pyrimidine motif triplex formation at neutral pH by more than 10-fold. It has also revealed that the interrupted 2′,4′-BNA^{NC} modification of TFO significantly increased the nuclease resistance of TFO in human serum. Selection of the interruptedly 2′,4′-BNA^{NC}-modified positions in TFO was more favorable for achieving the higher binding affinity of the pyrimidine motif triplex formation at neutral pH and the higher nuclease resistance of TFO than that of the continuously 2′,4′-BNA^{NC}-modified positions in TFO. We conclude that the design of TFO to bridge different positions of sugar moiety with polar atom-containing alkyl chain, and the introduction of such chemical modification into not continuous but interrupted positions in TFO are certainly promising strategies for the promotion of the pyrimidine motif triplex formation under physiological condition, and may eventually lead to progress in various triplex formation-based strategies in vivo, such as regulation of gene expression by antigene technology, mapping of genomic DNA, and gene-targeted mutagenesis.

REFERENCES

1. Chin, J.Y.; Schleifman, E.B.; Glazer, P.M. Repair and recombination induced by triple helix DNA. *Front. Biosci.* **2007**, 12, 4288–4297.
2. Bissler, J.J. Triplex DNA and human disease. *Front. Biosci.* **2007**, 12, 4536–4546.
3. Duca, M.; Vekhoff, P.; Oussedik, K.; Halby, L.; Arimondo, P.B. The triple helix: 50 years later, the outcome. *Nucleic Acids Res.* **2008**, 36, 5123–5138.
4. Jain, A.; Wang, G.; Vasquez, K.M. DNA triple helices: Biological consequences and therapeutic potential. *Biochimie* **2008**, 90, 1117–1130.
5. Wells, R.D. DNA triplexes and Friedreich ataxia. *FASEB J.* **2008**, 22, 1625–1634.
6. Frank-Kamenetskii, M.D. Protonated DNA structures. *Methods Enzymol.* **1992**, 211, 180–191.

7. Singleton, S.F.; Dervan, P.B. Influence of pH on the equilibrium association constants for oligodeoxyribonucleotide-directed triple helix formation at single DNA sites. *Biochemistry* **1992**, 31, 10995–11003.
8. Shindo, H.; Torigoe, H.; Sarai, A. Thermodynamic and kinetic studies of DNA triplex formation of an oligohomopyrimidine and a matched duplex by filter binding assay. *Biochemistry* **1993**, 32, 8963–8969.
9. Milligan, J.F.; Krawczyk, S.H.; Wadwani, S.; Matteucci, M.D. An anti-parallel triple helix motif with oligodeoxynucleotides containing 2′-deoxyguanosine and 7-deaza-2′-deoxyxanthosine. *Nucleic Acids Res.* **1993**, 21, 327–333.
10. Cheng, A.J.; Van Dyke, M.W. Monovalent cation effects on intermolecular purine-purine-pyrimidine triple-helix formation. *Nucleic Acids Res.* **1993**, 21, 5630–5635.
11. Lee, J.S.; Woodsworth, M.L.; Latimer, L.J.; Morgan, A.R. Poly(pyrimidine). poly(purine) synthetic DNAs containing 5-methylcytosine form stable triplexes at neutral pH. *Nucleic Acids Res.* **1984**, 12, 6603–6614.
12. Povsic, T.J.; Dervan, P.B. Triple Helix Formation by Oligonucleotides on DNA Extended to the Physiological Ph Range. *J. Am. Chem. Soc.* **1989**, 111, 3059–3061.
13. Xodo, L.E.; Manzini, G.; Quadrifoglio, F.; van der Marel, G.A.; van Boom, J.H. Effect of 5-methylcytosine on the stability of triple-stranded DNA—a thermodynamic study. *Nucleic Acids Res.* **1991**, 19, 5625–5631.
14. Ono, A.; Tso, P.O.P.; Kan, L.S. Triplex formation of oligonucleotides containing 2′-O-methylpseudoisocytidine in substitution for 2′-deoxycytidine. *J. Am. Chem. Soc.* **1991**, 113, 4032–4033.
15. Krawczyk, S.H.; Milligan, J.F.; Wadwani, S.; Moulds, C.; Froehler, B.C.; Matteucci, M.D. Oligonucleotide-mediated triple helix formation using an N3-protonated deoxycytidine analog exhibiting pH-independent binding within the physiological range. *Proc. Natl. Acad. Sci. USA* **1992**, 89, 3761–3764.
16. Koh, J.S.; Dervan, P.B. Design of a nonnatural deoxyribonucleoside for recognition of Gc base-pairs by oligonucleotide-directed triple helix formation. *J. Am. Chem. Soc.* **1992**, 114, 1470–1478.
17. Jetter, M.C.; Hobbs, F.W. 7,8-Dihydro-8-oxoadenine as a replacement for cytosine in the third strand of triple helices. triplex formation without hypochromicity. *Biochemistry* **1993**, 32, 3249–3254.
18. Ueno, Y.; Mikawa, M.; Matsuda, A. Nucleosides and nucleotides. 170. Synthesis and properties of oligodeoxynucleotides containing 5-[N-[2-[N,N-bis(2-aminoethyl)-amino]ethyl]carbamoyl]-2′-deoxyuridine and 5-[N-[3-[N,N-bis(3-aminopropyl) amino]propyl]carbamoyl]-2′-deoxyuridine. *Bioconjug. Chem.* **1998**, 9, 33–39.
19. Sun, J.S.; Giovannangeli, C.; Francois, J.C.; Kurfurst, R.; Montenay-Garestier, T.; Asseline, U.; Saison-Behmoaras, T.; Thuong, N.T.; Helene, C. Triple-helix formation by alpha oligodeoxynucleotides and alpha oligodeoxynucleotide-intercalator conjugates. *Proc.Natl.Acad.Sci.USA* **1991**, 88, 6023–6027.
20. Mouscadet, J.F.; Ketterle, C.; Goulaouic, H.; Carteau, S.; Subra, F.; Le Bret, M.; Auclair, C. Triple helix formation with short oligonucleotide-intercalator conjugates matching the HIV-1 U3 LTR end sequence. *Biochemistry* **1994**, 33, 4187–4196.
21. Rahman, S.M.; Seki, S.; Obika, S.; Haitani, S.; Miyashita, K.; Imanishi, T. Highly stable pyrimidine-motif triplex formation at physiological pH values by a bridged nucleic acid analogue. *Angew Chem. Int. Ed. Engl.* **2007**, 46, 4306–4309.
22. Rahman, S.M.; Seki, S.; Obika, S.; Yoshikawa, H.; Miyashita, K.; Imanishi, T. Design, synthesis, and properties of 2′,4′-BNA(NC): a bridged nucleic acid analogue. *J. Am. Chem. Soc.* **2008**, 130, 4886–4896.
23. Lyamichev, V.I.; Mirkin, S.M.; Frank-Kamenetskii, M.D.; Cantor, C.R. A stable complex between homopyrimidine oligomers and the homologous regions of duplex DNAs. *Nucleic Acids Res.* **1988**, 16, 2165–2178.
24. Torigoe, H.; Ferdous, A.; Watanabe, H.; Akaike, T.; Maruyama, A. Poly(L-lysine)-graft-dextran copolymer promotes pyrimidine motif triplex DNA formation at physiological pH—Thermodynamic and kinetic studies. *J. Biol. Chem.* **1999**, 274, 6161–6167.
25. Torigoe, H.; Hari, Y.; Sekiguchi, M.; Obika, S.; Imanishi, T. 2′-O,4′-C-methylene bridged nucleic acid modification promotes pyrimidine motif triplex DNA formation at physiological pH: thermodynamic and kinetic studies. *J. Biol. Chem.* **2001**, 276, 2354–2360.
26. Torigoe, H. Thermodynamic and kinetic effects of N3′–>P5′ phosphoramidate modification on pyrimidine motif triplex DNA formation. *Biochemistry* **2001**, 40, 1063–1069.

27. Torigoe, H.; Maruyama, A. Synergistic stabilization of nucleic acid assembly by oligo-N3′–>P5′ phosphoramidate modification and additions of comb-type cationic copolymers. *J. Am. Chem. Soc.* **2005**, 127, 1705–1710.
28. Torigoe, H.; Sasaki, K.; Katayama, T. Thermodynamic and kinetic effects of morpholino modification on pyrimidine motif triplex nucleic acid formation under physiological condition. *J. Biochem.* **2009**, 146, 173–183.
29. Torigoe, H.; Maruyama, A.; Obika, S.; Imanishi, T.; Katayama, T. Synergistic stabilization of nucleic acid assembly by 2′-O,4′-C-methylene-bridged nucleic acid modification and additions of comb-type cationic copolymers. *Biochemistry* **2009**, 48, 3545–3553.
30. Langerman, N.; Biltonen, R.L. Microcalorimeters for biological chemistry: applications, instrumentation and experimental design. *Methods Enzymol.* **1979**, 61, 261–286.
31. Biltonen, R.L.; Langerman, N. Microcalorimetry for biological chemistry: experimental design, data analysis, and interpretation. *Methods Enzymol.* **1979**, 61, 287–318.
32. Wiseman, T.; Williston, S.; Brandts, J.F.; Lin, L.N. Rapid measurement of binding constants and heats of binding using a new titration calorimeter. *Anal. Biochem.* **1989**, 179, 131–137.
33. Torigoe, H.; Shimizume, R.; Sarai, A.; Shindo, H. Triplex formation of chemically modified homopyrimidine oligonucleotides: thermodynamic and kinetic studies. *Biochemistry* **1999**, 38, 14653–14659.
34. Edwards, P.R.; Gill, A.; Pollard-Knight, D.V.; Hoare, M.; Buckle, P.E.; Lowe, P.A.; Leatherbarrow, R.J. Kinetics of protein-protein interactions at the surface of an optical biosensor. *Anal. Biochem.* **1995**, 231, 210–217.
35. Bates, P.J.; Dosanjh, H.S.; Kumar, S.; Jenkins, T.C.; Laughton, C.A.; Neidle, S. Detection and kinetic studies of triplex formation by oligodeoxynucleotides using real-time biomolecular interaction analysis (BIA). *Nucleic Acids Res.* **1995**, 23, 3627–3632.
36. Manzini, G.; Xodo, L.E.; Gasparotto, D.; Quadrifoglio, F.; van der Marel, G.A.; van Boom, J.H. Triple helix formation by oligopurine-oligopyrimidine DNA fragments. Electrophoretic and thermodynamic behavior. *J. Mol. Biol.* **1990**, 213, 833–843.
37. Wickstrom, E. Oligodeoxynucleotide stability in subcellular extracts and culture media. *J. Biochem. Biophys. Methods* **1986**, 13, 97–102.
38. Cheng, Y.K.; Pettitt, B.M. Stabilities of double- and triple-strand helical nucleic acids. *Prog. Biophys. Mol. Biol.* **1992**, 58, 225–257.
39. Edelhoch, H.; Osborne, J.C., Jr. The thermodynamic basis of the stability of proteins, nucleic acids, and membranes. *Adv. Protein Chem.* **1976**, 30, 183–250.
40. Kamiya, M.; Torigoe, H.; Shindo, H.; Sarai, A. Temperature dependence and sequence specificity of DNA triplex formation: An analysis using isothermal titration calorimetry. *J. Am. Chem. Soc.* **1996**, 118, 4532–4538.
41. Shafer, R.H. Stability and structure of model DNA triplexes and quadruplexes and their interactions with small ligands. *Prog. Nucleic Acid Res. Mol. Biol.* **1998**, 59, 55–94.
42. Zon, G.; Geiser, T.G. Phosphorothioate oligonucleotides: chemistry, purification, analysis, scale-up and future directions. *Anticancer Drug Des.* **1991**, 6, 539–568.
43. Stein, C.A.; Tonkinson, J.L.; Yakubov, L. Phosphorothioate oligodeoxynucleotides–anti-sense inhibitors of gene expression? *Pharmacol. Ther.* **1991**, 52, 365–384.
44. Xodo, L.; Alunni-Fabbroni, M.; Manzini, G.; Quadrifoglio, F. Pyrimidine phosphorothioate oligonucleotides form triple-stranded helices and promote transcription inhibition. *Nucleic Acids Res.* **1994**, 22, 3322–3330.